Acoustical Characteristics of Textile Materials

Vijayanand S. Moholkar and Marijn M.C.G. Warmoeskerken

Textile Research Journal 2003; 73; 827
DOI: 10.1177/004051750307300914

Acoustical Characteristics of Textile Materials

VIJAYANAND S. MOHOLKAR[1] AND MARIJN M. C. G. WARMOESKERKEN

Textile Technology Group, Department of Chemical Engineering, University of Twente, 7500 AE Enschede, The Netherlands

ABSTRACT

An attempt is made to identify the acoustical characteristics of textile materials using precision woven monofilament fabrics as model textiles. The experiments try to eliminate the effect of entrapped air pockets in the fabric on an ultrasound wave field. The results of the experiment reveal that the power consumption of the ultrasound horn remains practically constant after introducing the textile at different positions in the standing wave field. Measurements of transmitted acoustic pressure amplitude through the textile reveal that fabrics form an almost transparent boundary for acoustic waves. A simple model involving the structural and hydrodynamic characteristics of the textiles is proposed to determine their acoustic impedance, and the results of the experiments are explained on the basis of this model. The overall conclusion of the study is that in the absence of entrapped air, textiles do not have any individual impact on the ultrasound wave field.

Textile processing industries are energy intensive. The dominant mass transfer mechanism in wet textile processes is molecular and convective diffusion in the interyarn and intrayarn pores of the textile. Wet textile processes, such as washing, dyeing, rinsing, desizing, mercerizing, and bleaching, which involve mass transfer inside the textile, suffer from two major drawbacks: They require large process times and have low energy efficiency. Intensification of mass transfer in textiles is of paramount importance for improving the efficiency of wet textile processes. A textile is basically a (bi)porous viscoelastic material made of either natural or synthetic fibers. Textiles can have either single (interyarn) porosity or dual (interyarn and intrayarn) porosity. However, due to the high flow resistance of intrayarn pores, most of the flow occurs in the interyarn region, with little or no flow in the intrayarn pores [18]. Therefore, the rate-controlling step in overall mass transfer in textile materials is diffusion in the intrayarn pores. Improving wet textile processes basically means converting this intrayarn diffusion to a faster convection process.

As a means of improving the efficiency of both chemical and physical processes, power ultrasound has been attempted in the last several years (for details see references 16, 17). Recently, ultrasound has also been used to intensify mass transfer in wet textile processing. McCall *et al.* [9] reported improved dye uptake in the fabric in the presence of ultrasound. Yachmenev *et al.* [20, 21] demonstrated improved efficiency of enzymatic treatments of fabric, such as bioscouring, with ultrasound. Rathi *et al.* [15] reported enhanced efficiency of open width washing of fabrics with ultrasound. Despite encouraging results from laboratory scale studies, the interests of the process industries have not yet been served by the ultrasound-based technology. Two major factors contributing to this fact are the lack of precise knowledge about the mechanisms of ultrasound-assisted processes and their inherent drawbacks, such as the directional sensitivity of ultrasound effects, erosion of the sonicator surface, and non-uniform volumetric energy density at optimal cavitation conditions. Recently, we showed [10, 11] that transient cavitation in a medium (*i.e.*, water) close to the textile surface is the basic physical mechanism of ultrasonic mass transfer intensification in textiles. Intense microturbulence generated by the transient radial motion of bubbles close to the textile surface is responsible for generating intrayarn convection that enhances mass transfer in the textile. Although establishing the physical mechanism of ultrasonic wet textile treatments is an important step toward their implementation on an industrial scale, the secondary aspects of this technology need to be investigated before achieving the final goal. One such aspect is the acoustic characteristics of textile materials.

Acoustically, porous materials are categorized as sheet materials and bulk materials on the basis of their thickness compared to the wavelength of sound. Sheet materials are those with a much smaller thickness than the

[1] Author to whom correspondence should be addressed: "Karishma", 2/A, Pramod Housing Society, Vijapur Road, Solapur 413 004, Maharashtra, India, e-mail: vmoholkar@rediffmail.com

0040-5175/$15.00

wavelength of sound, while the thickness of the bulk materials is much larger than the wavelength of sound. The acoustic behavior of sheet materials is controlled by viscous effects and area density (mass per unit area), while viscous and thermal effects and the solid material density control the acoustic behavior of bulk materials.

In this paper, we attempt to discern the acoustic characteristics of different textile materials. The parameters that form the basis of our acoustic characterization of textiles in this study are attenuation of the acoustic wave by textile materials and the acoustic impedance of textile materials. These two parameters are related to each other, however, as we will discuss in greater detail in the text. Since this study is part of our attempt to investigate the physical mechanism of ultrasonically enhanced wet textile processes, we have used water as the medium for ultrasound.

Previous Work

The acoustic properties of porous sheet materials have been investigated throughout the past several decades. The principal contributions in this area were made by Beranek [1, 2], Nichols [12], Zwikker and Kosten [22], Bies [3], and Vér and Holmer [19]. A large amount of literature on this subject has accumulated over the past decades.

Attempts to determine the acoustic characteristics of textile materials, however, are few. Datar *et al.* [4, 5] studied the attenuation of ultrasound through textile materials for low and high intensity ultrasound. They reported the effect of several parameters, such as fabric weight, ultrasound frequency, fiber type, and wetting of the textile surface, on the attenuation of ultrasound as it passes through the fabric. Datar *et al.*'s study, despite its thoroughness, has several questionable conclusions.

The acoustic wave, during its passage through water, can also be attenuated by bubbles in the water if the water has not been completely degassed. A rigorous treatment of the problem of acoustic wave propagation through bubbly liquids was given by Prosperetti and Commander [14]. During radial oscillations of the bubbles driven by an acoustic wave, bubble size distribution can change as a result of rectified diffusion, which is a process of gas transport in and out of bubbles. A rigorous treatment of the problem of rectified diffusion during radial bubble motion was reported by Fyrillas and Szeri [7]. For greater details on acoustic wave propagation in bubbly liquids and rectified diffusion, we refer the reader to these papers, but we state here the major conclusions of these papers, which are relevant to our study. The extent of wave attenuation by bubbles is determined by two factors: the bubble population and the size of the bubbles. Whether the bubbles will grow or shrink as a result of rectified diffusion is determined by the dissolved gas content of the medium, the pressure amplitude and frequency of the acoustic wave, and the initial size of the nuclei from which the bubbles grow. In order to determine the acoustic characteristics of textile materials by acoustic wave attenuation, it is necessary to isolate these effects of gas bubbles.

In their experiments, Datar *et al.* [4, 5] used water that was not completely degassed as the medium. In addition, they conducted experiments at acoustic pressure amplitudes higher than the transient cavitation threshold. Under the conditions of their experiments, it was very difficult to distinguish the effect of cavitation bubbles and of fabric properties on ultrasound attenuation. Therefore, their results are questionable in terms of the acoustic properties of the textiles alone.

In this study, we attempt to deduce the acoustic characteristics of textile materials while excluding the secondary effects due to cavitation bubbles. For this purpose, we use two methods: raising the static pressure of the experimental system well above the pressure amplitude of the ultrasound wave, which results in suppression of cavitation, and using precision woven monofilament textiles in which the intrayarn pores, which can entrap gas pockets that provide nuclei for cavitation in the vicinity of the textiles, are absent.

The Physical Model

Transmission Loss Through Porous Sheet Materials

A complete list of our notation is given in Appendix B, and a general description of the problem of plane wave reflection at a surface is given in Appendix B. When an acoustic wave is incident on a sheet material, such as a thin slab or a plate, a fraction of the wave energy is reflected and the rest is transmitted. In this situation, the sound-power transmission coefficient is defined as the ratio of the transmitted sound power to the incident sound power. If the incident wave is a plane wave, and if the structural properties of the slab do not change in the direction of wave propagation, the transmitted wave will also be a plane wave traveling in the same direction as the incident wave (Pierce [13]). The transmission loss coefficient is defined as

$$R_{TL} = 10 \log (1/\tau) \quad , \tag{1}$$

where τ is the ratio of mean squares of the pressure amplitudes of the transmitted wave (P_T) and the incident wave (P_I) (Vér and Holmer [19]). In other words, τ is

equal to the square of the transmission coefficient of the acoustic wave, as described in Appendix B.

If the properties of the sheet are such that the oscillatory velocities of the fluid elements on the two sides of the sheet v_f and v_b are equal, then the analysis of acoustic wave transmission can be simplified (Pierce [13]). In the case of a porous sheet, this condition holds true if the pore volume per unit area of the sheet is substantially less than a quarter of the wavelength of the acoustic wave. This hypothesis is based on two assumptions. First, density variation in the pores of the sheet is not much different from density variation in the bulk fluid on both sides of the sheet. Second, although the velocity of the fluid in individual pores is different from the inlet or outlet velocity, these variations are smoothed out if the velocities of the fluid elements are averaged over a large area of the sample.

Consider an acoustic wave incident on a porous sheet, as shown in Figure 1. Using the basic definition of the acoustic impedance (Z) in terms of the acoustic pressure (p) and velocity (v), *i.e.*, $Z = p/v$, we can write

$$P_f - P_b = Z_s v_f = Z_s v_b \quad , \tag{2}$$

where P_f and P_b are the pressures at the front and back sides of the slab, and v_f and v_b are the corresponding fluid velocities. Z_s is the specific acoustic impedance of the porous sheet. Dividing Equation 2 by $v_f = v_b = v$, we obtain

$$Z_f = Z_b + Z_s \quad . \tag{3}$$

This is analogous to an electric circuit where the combined or resultant impedance of two elements in a series is the summation of their individual impedances. The pressure-amplitude transmission coefficient can now be calculated.

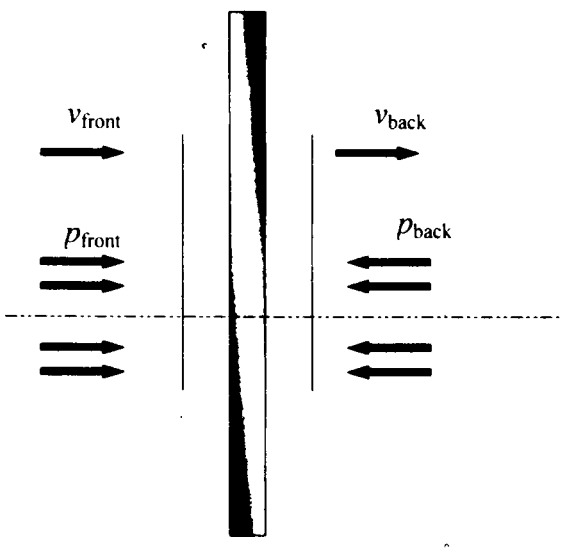

FIGURE 1. Interaction of an acoustic wave with a thin porous sheet.

The pressure-amplitude reflection coefficient for a sound wave incident on an interface between two media, as described in Appendix B, is

$$R = \frac{Z_2 - Z_1}{Z_2 + Z_1} \quad . \tag{4}$$

The pressure on the front side of the fabric is the pressure of the incident wave (P_I) minus the pressure of the reflected component of the incident wave (RP_I). Therefore, by the definition of acoustic impedance just stated, the velocity on the front side of the sheet is

$$v_f = \frac{P_I}{Z_I}(1 - R) \quad . \tag{5}$$

Setting $Z_2 = (Z_s + Z_I)$ and $Z_1 = Z_I$, we get

$$v_f = \frac{2P_I}{2Z_I + Z_s} \quad . \tag{6}$$

At the rear side of the slab, the phase or medium is homogeneous. The acoustic pressure in this region is the transmitted component of the incident wave (P_T). Again, using the basic definition of acoustic impedance, we have

$$P_T = Z_I v_b \quad . \tag{7}$$

Since $v_f = v_b$, the pressure-amplitude transmission coefficient is

$$\tau = \frac{P_T}{P_I} = \frac{2Z_I}{2Z_I + Z_s} \quad . \tag{8}$$

The transmission loss coefficient is now calculated using Equation 1:

$$R_{TL} = 10 \log\left(\left|1 + \frac{Z_s}{2Z_I}\right|^2\right) \quad . \tag{9}$$

In order to calculate the transmission loss coefficient, we need to determine the specific acoustic impedance of the porous sheet Z_s. In the next section, we present a simple model for this purpose.

SPECIFIC ACOUSTIC IMPEDANCE OF A POROUS SHEET

Consider a porous sheet on which an acoustic wave is incident, as shown in Figure 1. For a steady oscillatory flow, the transverse velocity in the bulk on either side of the sheet (relative to the velocity of the sheet itself, *i.e.*, v_s) is (Pierce [13])

$$v_f - v_s = v_b - v_s = \frac{1}{R_f}(P_f - P_b) \quad . \qquad (10)$$

This relation is analogous to an electric circuit, where the velocity and pressure difference are the counterpart of the current and voltage, respectively. The flow resistance of the porous sheet (R_f) can be determined by holding the sheet fixed and forcing the liquid through it at a known rate, then measuring the pressure drop across the textile.

If the porous sheet is moving freely, on the basis of Newton's law (rate of change of momentum is directly proportional to the applied force), we can write

$$m_s \frac{\partial v_s}{\partial t} = (P_f - P_b) \quad . \qquad (11)$$

Substitution for v_s gives

$$m_s \frac{\partial}{\partial t}\left(v_f - \frac{1}{R_f}(P_f - P_b)\right) = (P_f - P_b) \quad . \qquad (12)$$

Setting $\partial/\partial t \sim -i\omega$ and dividing by $(P_f - P_b)$, we have

$$-i\omega m_s \frac{v_f}{(P_f - P_b)} + \frac{1}{R_f} i\omega m_s = 1 \quad . \qquad (13)$$

Substituting $\frac{v_f}{(P_f - P_b)} = Z_s$ from Equation 2 gives

$$\frac{1}{Z_s} = \frac{-1}{i\omega m_s} + \frac{1}{R_f} \quad , \qquad (14)$$

and a simplification of this expression gives

$$Z_s = \frac{R_f(\omega m_s)^2 - iR_f^2(\omega m_s)}{R_f^2 + (\omega m_s)^2} \quad . \qquad (15)$$

For two limit cases, depending on the relative magnitudes of R_f and ωm_s, the expression for Z_s can be reduced to

$$Z_s = -i\omega m_s \quad \text{for } \omega \ll R_f/m_s \quad , \qquad (16a)$$

$$= R_f \quad \text{for } \omega \gg R_f/m_s \quad . \qquad (16b)$$

The transmission loss coefficient (in dB) for a porous sheet can be calculated by substituting Equation 16 into Equation 9 for the two limit cases mentioned above.

Experimental

The experimental system in this study has two sections: the ultrasound system and the flow resistance measurement unit. Descriptions of each unit and operational procedures are given below.

ULTRASOUND SYSTEM

The ultrasound system has three main components: an experimental cell, a high pressure vessel, and an ultrasound horn, along with a signal generator and amplifier. A schematic diagram of the set-up is shown in Figure 2.

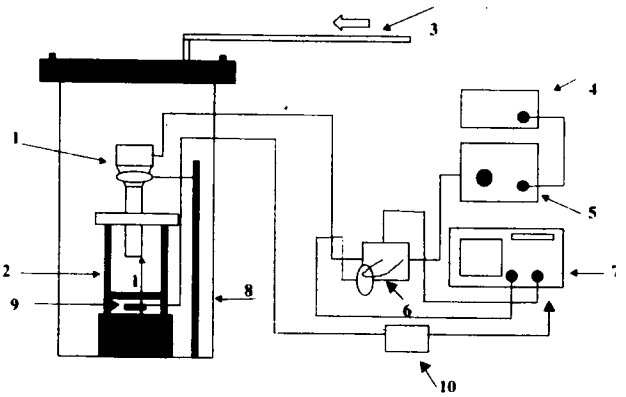

FIGURE 2. Schematic diagram of the experimental set-up in the ultrasound unit: (1) ultrasound horn, (2) experimental cell with textile sample, (3) compressed air (7 bar), (4) signal generator, (5) RF amplifier, (6) voltage and current monitoring unit, (7) digital oscilloscope, (8) high-pressure vessel, (9) hydrophone, (10) charge amplifier.

The Experimental Cell

The experimental cell is made of three detachable glass rings and a Teflon lid. The height of the two rings is 15 mm, which corresponds to one-quarter of the wavelength of 25 kHz ultrasound (60 mm) in water, while the height of the third ring is 60 mm. The cell is mounted on a 51 mm thick stainless steel bottom, with four vertical bars that act as supports for the glass rings placed above each other. The stainless steel bottom of the experimental cell acts as a rigid reflector for the ultrasound waves. The cell has calibrated distance marks on it to measure the distance between the ultrasound horn tip and the rigid bottom. A textile sample can be placed between the glass rings at a certain distance from the bottom, and the glass rings can be pressed together with the lid on the top of the third ring. Rubber gaskets are placed between the textile and glass rings in order to avoid leakage. At the bottom of the cell, there is a special arrangement for placing the hydrophone (Bruel & Kæjer Ltd., type 8103) to measure the acoustic pressure amplitude. The output of the hydrophone is transformed into proportional voltage by a charge amplifier (Nexus Range, model 2690), and this voltage is monitored on a digital oscilloscope (Tektronics Ltd., model 430A).

The Ultrasound Unit

The ultrasound unit consists of a special ultrasound horn with a central resonance frequency of 25 kHz when vibrating in air. The horn has the ability to cool the piezoelectric element during operation in order to keep its temperature constant. The horn is driven by a signal generator (Hewlett-Packard Inc., model 3324A) and a radio frequency amplifier (ENI Inc., model 2100L). The amplifier can supply a maximum of 200W of electrical power for a large frequency range (10 kHz to 1 MHz) for an input-impedance of 50Ω. The output power of the amplifier is controlled by adjusting the input signal voltage to the amplifier (maximum allowed input signal voltage, 1 V_{p-p}). The signal generator can supply signals in the frequency range of 1 mHz to 21 MHz, with voltage up to 3.5 V_{rms} (at an output impedance of 50Ω). The voltage and frequency of the signal generated by the signal generator can be varied in steps of 1 mV and 1 mHz, respectively. Thus, both the voltage and the frequency of the input signal to the amplifier and, hence, the electrical power consumption of the ultrasound horn can be precisely controlled for different sets of experiments with varying process parameters. The voltage and current supplied to the ultrasound horn are monitored with a voltage probe (Tektronics Ltd., model 6138A) and a current clamp (Farnell Inc., model PR-20). The peak-to-peak voltage (V_{p-p}), peak-to-peak current (I_{p-p}), and phase angle (ϕ) between them are measured with a digital oscilloscope, and the power consumed by the ultrasound horn can be calculated from these measurements:

$$\text{Power} = \frac{V_{p-p} I_{p-p} \cos \phi}{4} \quad . \qquad (17)$$

The ultrasound horn is mounted onto the shaft of a laboratory jack, and the experimental cell is placed on its base. The base of the jack can be raised or lowered to adjust the distance between the bottom of the cell and the tip of the horn.

The Pressure Vessel

In order to conduct experiments at raised static pressure, we have constructed a high-pressure vessel (volume 40 L, maximum working pressure 10 bar) to accommodate the jack with the ultrasound horn mounted on the shaft and the experimental cell placed on the base. The pressure vessel is equipped with electrical connections for the ultrasound horn, the hydrophone connections, and a safety release valve.

We must specifically mention that since the diameter of the cell is 60 mm and the diameter of the ultrasound horn tip is 30 mm, the standing wave field generated in the cell does not have exact planar characteristics: a small residual pressure amplitude exists at the velocity antinode, while a small residual velocity amplitude exists at the pressure antinode. This non-ideal set-up needs to be remembered when interpreting the results of the experiments, which use the position of the fabric in the standing wave field as a parameter.

FLOW RESISTANCE MEASUREMENT UNIT

The schematic diagram of the set-up for flow resistance measurements of textile materials is shown in Figure 3. The set-up comprises two circular columns 50 mm in diameter and approximately 50 cm long (made of acrylic material), between which the textile sample is fixed during experiments. A thin rubber gasket is placed on the textile to avoid leakage. A 50 L plastic tank is used as water reservoir, and an Iwaki-MD6 pump (maximum output 38 L/minute) is used to circulate water in the flow loop. The flow through the column (and hence through the textile) is measured with help of two GF rotameters (one with a range of 5–50 L/hour and the other 30–300 L/hour). The pressure difference across the textile sample is measured with a Honeywell STD-120 differential pressure indicator. Air locks are provided on the tubes connecting the acrylic columns to the pressure indicator in order to isolate the flow loop to the pressure indicator from the main flow loop during replacement of samples. This prevents admittance of any air bubble into the pressure indicator flow loop, which can hinder accurate measurement of the pressure drop across the textile. The pressure indicator is calibrated against a water manometer according to the calibration chart shown in Figure 4. The maximum pressure drop range of the pressure indicator is 200 mbar, with a resolution of 0.2 mbar.

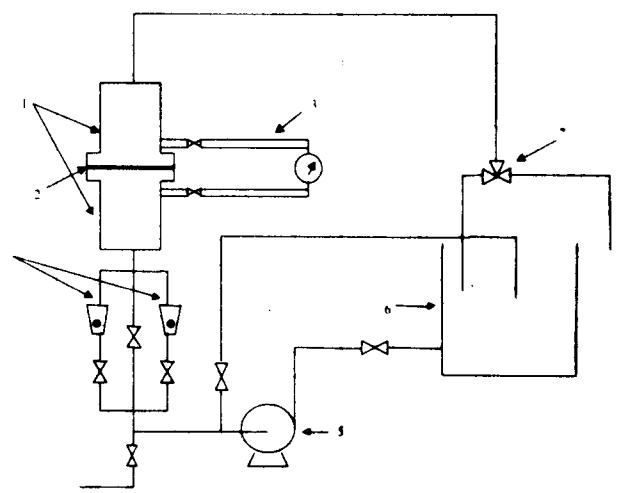

FIGURE 3. Schematic diagram of the experimental set-up for flow resistance measurements: (1) detachable columns to hold the textile, (2) textile sample, (3) pressure transmitter with air locks, (4) rotameters, (5) pump, (6) water reservoir, (7) 3-way valve for collecting samples for the analysis.

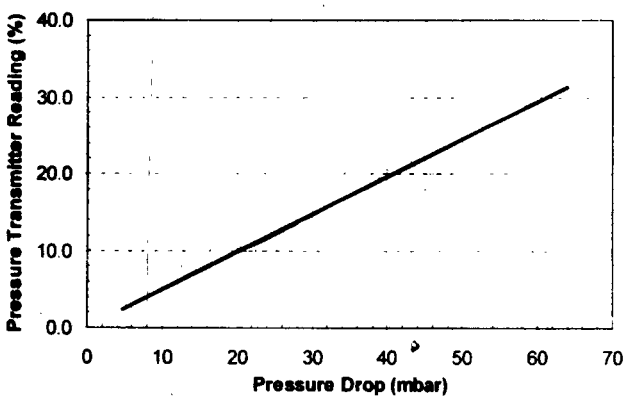

FIGURE 4. Calibration of the pressure indicator. The *X*-axis represents the absolute pressure drop while *Y*-axis indicates the pressure indicator reading.

MODEL TEXTILES

Polyamide monofilament precision woven screening fabrics are the model textiles. These monofilament textiles have only a single porosity, *i.e.*, interyarn porosity, and were obtained from Sefar Inc. (Filtration Division), Switzerland. Seven samples with different specifications were selected, and their detailed specifications are given in Table I.

EXPERIMENTAL PROCEDURE

Ultrasound Experiments

The amplitude of the acoustic wave generated by the ultrasound horn was measured with only water in the experimental cell (without textile) as 1.2 bar. This value was regarded as the *reference* or (un-attenuated) incident acoustic pressure amplitude. (Note that due to the formation of standing waves in the cell, the acoustic pressure amplitude is doubled, so the reference acoustic pressure amplitude of 1.2 bar corresponds to traveling acoustic waves with an amplitude of 0.6 bar.) We determined the power consumption of the ultrasound horn for these conditions using the voltage and current measurements on the digital oscilloscope. This power consumption value was regarded as the *reference* power value. In subsequent experiments, the textile sample was placed between the rings of the experimental cell (at either the pressure antinode or the pressure node) inside a water bath to avoid trapping air below the textile surface. The quantity of de-mineralized water in the cell was fixed at 250 ml, and the distance between the ultrasound horn tip and the bottom of the experimental cell was fixed at 6 cm (which is the wavelength of 25 kHz ultrasound wave in water). This apparatus was placed inside the high-pressure vessel, and the pressure was raised to 6.5 bar. The apparatus was then kept pressurized for approximately 1 hour to minimize the effect of gas bubbles present in the medium. Later, the ultrasound was turned on (with a signal input of 50 mV_{rms} to the amplifier), with the experimental apparatus still pressurized at 6.5 bar. (Conducting the experiments under high static pressure helped completely remove the effect of attenuation due to bubbles.) The voltage and current supplied to the ultrasound horn were monitored on the digital oscilloscope, and the frequency of the ultrasound was tuned slightly to remove the phase angle between the voltage and current. In order to measure the attenuation of the acoustic wave by the textile, the power consumption of the ultrasound horn was re-adjusted to the

TABLE I. Specifications of Sefar model textiles.

Sample	Mesh opening, μm	Open area, %	Mesh count, warp/weft, n/cm	Wire dia., μm, warp	Wire dia., μm, weft	Weight, g/m^2	Thickness, μm
03-20/14	20	14	188/188	34	34	35	55
03-30/20	30	20	150/150	40	40	35	70
03-48/26	48	25.5	106/106	47	47	35	75
03-41/31	41	31	136/136	33	33	25	50
03-63/30	63	30	78/94	43	43	35	95
03-53/30	53	30	144/104	43	43	43	100
03-35/16	35	16	100/128	43	43	49	97

Sample	Mass reactance (imaginary component of Z_s), kg m^{-2} s^{-1}	Specific flow resistance (real component of Z_s), Pa-s m^{-1}
03-20/14	5497	12408
03-30/20	5497	12079
03-48/26	5497	4272
03-41/31	3927	2733
03-63/30	5497	2802
03-53/30	6754	4249
03-35/16	7697	8643

reference value (by slightly changing the signal input to the amplifier), and the amplitude of the acoustic wave sensed by the hydrophone was noted.

Flow Resistance Measurement

The acrylic columns were fixed together without the textile, and water was circulated in the flow loop for about half an hour (with all the valves opened except the bypass valve and the holdup-removal valve) to completely remove air trapped in the loop. Once no air bubbles were visible in the water flow in the columns, the flow in the columns was allowed only through one rotameter (30–300 L/hour), with all the other valves closed. The air locks in the flow loop of the pressure indicator were closed before the columns were opened to remove or replace the textile sample. The textile samples were thoroughly wetted before they were placed between the columns, so as to remove any air trapped in the interyarn pores. We especially tried to avoid any entrapment of air bubbles beneath the textile surface, which could hamper the accurate measurement of the pressure drop. A small amount of chlorine bleaching agent was added to avoid any bacterial growth in the water reservoir during storage.

Results and Discussion

The theory of the equivalent circuit of a piezoelectric transducer states that the electrical power consumed by the transducer is a function of the specific acoustic impedance of the medium in which it is oscillating (Ensminger [6]). In this case, the impedance a piezoelectric transducer encounters for oscillatory motion is the sum of the acoustic impedance of the medium and the acoustic impedance of the textile sample given by Equation 2.

The power consumption of the ultrasound horn with the textile positioned at the pressure node and the pressure antinode in the standing wave field are shown in Figure 5. The reference power value, which is the power consumption of the ultrasound horn with only water as the medium, is also shown in these figures. The sound-power transmission loss calculated using experimentally measured values of incident and transmitted acoustic pressure amplitudes for a textile positioned at the pressure node and the pressure antinode are shown in Figure 6. The flow resistance of the textile samples can be found from the slope of the plot of pressure drop versus liquid velocity, which is linear in the laminar flow regime (Gooijer [8]). A typical graph of pressure drop versus liquid velocity is shown in Figure 7, along with the flow resistance, which is the slope of the graph. Flow resistance values of all other fabrics determined in a similar way are listed in Table I. We can infer from Figure 5 that the presence of the textile in the standing wave causes a negligible change to the power consumption of the ultrasound horn. This is indicative of the fact that the total acoustic impedance of the system remains practically constant after placing the textile in the standing wave field generated in the experimental cell. Explanations for these results can be given on the basis of the physical model for the acoustic impedance of the textile materials presented earlier in this section.

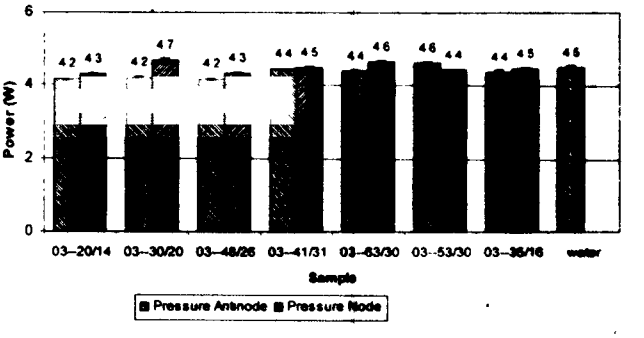

FIGURE 5. Power consumption of the ultrasound horn with placement of different textile samples in the standing wave field.

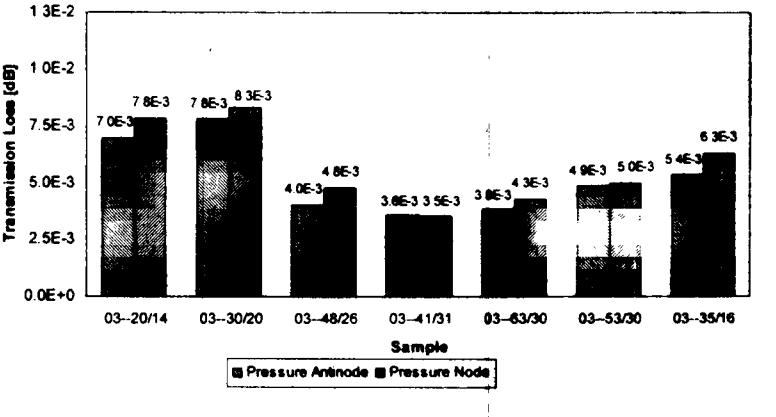

FIGURE 6. Experimental sound-power loss coefficients (R_{TL}) for different textile samples at different positions in the standing wave field.

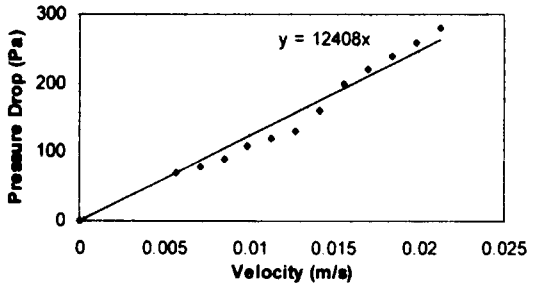

FIGURE 7. Flow resistance measurement for textile sample 03-20/14. (Values of specific flow resistances for all samples determined in similar way are listed in Table I.)

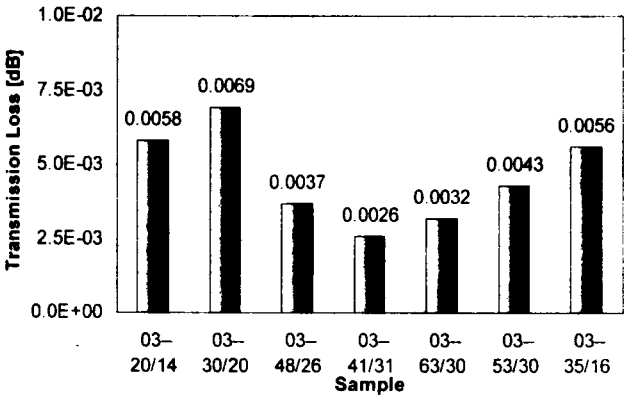

FIGURE 9. Theoretical sound-power transmission loss for different textile samples.

The two components of the acoustic impedance of the textile are the flow resistance (the real part, independent of the frequency of the acoustic wave) and mass reactance (the imaginary part, which is a function of the frequency of the acoustic wave). The individual values of these two components are listed in Table I, and the resultant acoustic impedances for different textile samples, determined using Equation 14, are shown in Figure 8. The medium for ultrasound used in these experiments is water, whose acoustic impedance ($Z_l = \rho c$, $\rho = 1000$ kg m^{-3}, $c = 1500$ m s^{-1}) is 1.5×10^6 kg m^{-2} s^{-1}. The specific acoustic impedance of all the samples shown in Figure 8 is much smaller than the acoustic impedance of the medium itself. Therefore, the impedance of the experimental cell remains practically constant after introducing the textile sample, thus causing no change in the power consumption of the ultrasound horn. The results shown in Figure 8 along with Equation 16 also help determine the theoretical sound-power transmission loss coefficients for the acoustic waves, shown in Figure 9 for model textiles. The experimental and theoretical values of sound power transmission loss coefficients (shown in Figures 6 and 9, respectively) match to a fair degree. The experimental values show that the textile transmits practically all the energy of the acoustic wave incident on it. This result can be explained on the basis of the ratio of the acoustic impedance of the textile and that of the medium. One can easily perceive from the Z_s values reported in Figure 8 that the ratio $(Z_s/Z_l) \sim 10^{-3}$ or so. Therefore, the transmission loss coefficient as defined by Equation 9 is very small, on the order of 10^{-4} or so. This justifies the experimental values of sound-power transmission loss coefficient and the conclusion that textiles form an almost transparent boundary for acoustic waves with water as the medium. Note, however, that if the medium for ultrasound changes, for example, from water in our study to air, this conclusion is subject to variation.

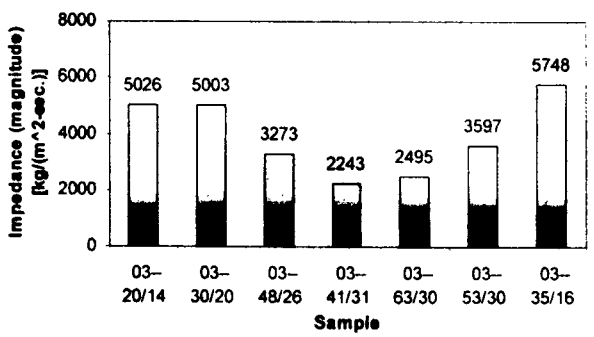

FIGURE 8. Magnitude of acoustic impedance of textile samples calculated using Equation 14.

Conclusions

Our study proposes a simple methodology for determining the acoustic characteristics of textile materials with water as the medium for ultrasound. The experimental techniques used in this study separate out the effect of entrapped air pockets (or air bubbles) in the textile, thus revealing the individual effect of the textile on the ultrasound wave field. The theoretical model for acoustic impedance of the textile reveals that it is determined by both structural (mass per unit area) and hydrodynamic (specific flow resistance) properties of the textile material. The mass per unit area and flow resistance act as two resistances in parallel. The presence of the textile material causes practically no change in the acoustic impedance of the system and, hence, in the power consumption of the ultrasound horn. Consistent with this result, measurements of the pressure amplitude of the acoustic waves passing through the textile reveal that the textile materials form a practically transparent boundary for

coustic waves with water as the medium, transmitting nost of the acoustic energy incident on them. Theo-etically predicted and experimentally determined ound power transmission loss coefficients match to a air degree and are of the order $\sim 10^{-4}$. This also neans that attenuation of the acoustic waves by tex-iles, as observed in practice, is the secondary effect of ir pockets trapped in the textiles. Another conclusion lrawn from this study is that ultrasound enhancement of wet textile treatments is also an effect of air pockets rapped in the textile (for greater details on the mech-nistic and process engineering aspects of ultrasonic vet textile treatments, the reader is referred to Mohol-ar [10]).

We have verified the validity of this conclusion in experiments with several commercial textiles of different properties. In these experiments, we have measured only he change in power consumption of the ultrasound horn fter placing the textile at the pressure node and the pressure antinode in the standing wave field. The results of the experiments are shown in Figure 10, along with he reference power value. Figure 10 reveals that the presence of the textile in the standing wave field does not ause any significant change in the power consumption of the ultrasound horn. This result confirms the validity of our conclusions for commercial textiles.

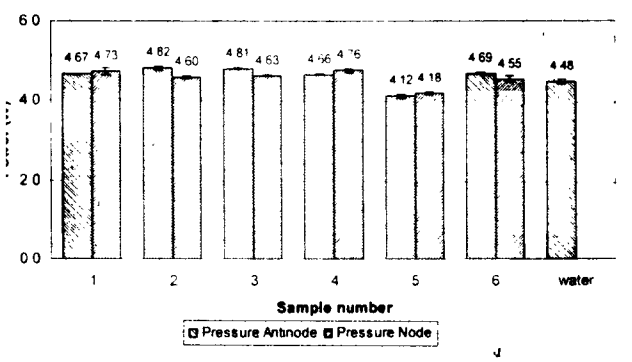

FIGURE 10. Variation in power consumption of ultrasound horn with resence of commercial textile in standing wave field at different ositions. Description of samples with numbers: (1) Ten Cate sample B cotton, 207 g/m^2), (2) Ten Cate sample C (cotton, 196 g/m^2), (3) Ten ate sample D (cotton, 185 g/m^2), (4) Vlisco 4212 (cotton, 112 g/m^2), 5) Vlisco 4350 (cotton, 118 g/m^2), (6) Ten Cate cotton polyester cotton 60%—polyester 40%, 580 g/m^2).

ACKNOWLEDGMENTS

We would like to thank Stork Brabant B. V. Boxmeer, Netherlands) for funding the project at the Jniversity of Twente. We also thank Sefar Inc., TNO-Textile, and Royal Ten Cate for providing the textile amples. V. S. Moholkar is grateful to Dr. ir. Henk Gooijer and Mr. Rene Breeuwer (TNO-TPD, Delft, Netherlands) for their help in this work.

Appendix A

NOTATION

c velocity of sound, m s^{-1}
m_s mass per unit area of the porous sheet, kg m^{-2}
P_b acoustic pressure on the back side of the slab, Pa
P_f acoustic pressure on the front side of the slab, Pa
P_I acoustic pressure amplitude of the incident wave, Pa
P_T acoustic pressure amplitude of the transmitted wave, Pa
R pressure-amplitude reflection coefficient, dimensionless
R_f specific flow resistance of the porous slab, Pa-s m^{-1}
R_{TL} sound-power transmission loss, dB
v_b fluid velocity on the back side of the slab, m s^{-1}
v_f fluid velocity on the front side of the slab, m s^{-1}
v_s velocity of the porous sheet, m s^{-1}
Z_1 acoustic impedance of the first medium, Pa-s m^{-1}
Z_2 acoustic impedance of the second medium, Pa-s m^{-1}
Z_b acoustic impedance at the back side of the slab, Pa-s m^{-1}
Z_f acoustic impedance at the front side of the slab, Pa-s m^{-1}
Z_I acoustic impedance of the medium, Pa-s m^{-1}
Z_s acoustic impedance of a sheet, Pa-s m^{-1}

Greek Notation

ρ density of the medium, kg m^{-3}
τ sound-power transmission loss coefficient, dimensionless
ω angular frequency of the acoustic wave, rad s^{-1}

Appendix B

PLANE WAVE REFLECTION AT A SURFACE

If a wave strikes a surface or a boundary between two media during its propagation in a medium, a reflected wave is produced. This physical characteristics of the reflected wave depend on the characteristics of the surface and of the medium, or on the characteristics of the two media. We treat the general case, of a plane wave reflection at a boundary between two media with specific acoustic impedances $Z_I(\rho_I c_I)$ and $Z_{II}(\rho_{II} c_{II})$. The incident wave is now split into

two parts: first, a reflected wave back in the first medium, and second, a transmitted wave as shown in Figure 11. We assume that the boundary is massless and there is no loss of energy due to absorption or dissipation.

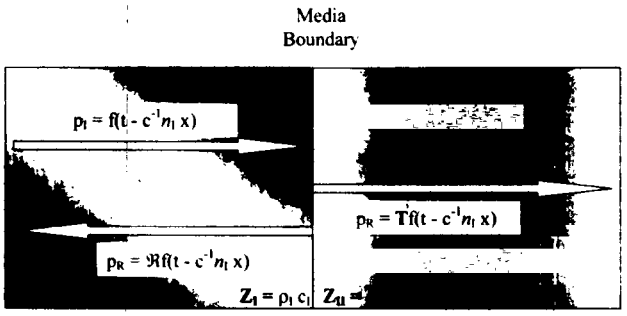

FIGURE 11. Reflection/transmission of an acoustic wave at a boundary between two media.

Let p_I, p_R, and p_T denote the pressure amplitudes of the incident, reflected, and transmitted acoustic waves, respectively. The ratio p_R/p_I is termed the reflection coefficient of the wave ($\Re$), while the ratio p_T/p_I is termed the transmission coefficient of the wave (**T**). At the boundary, there can be no discontinuity of pressure or of velocities. Using this argument, we can write

$$p_I = p_R + p_T \quad \text{or} \quad 1 - \Re = \mathbf{T} \quad , \qquad \text{(A1)}$$

$$\frac{1}{(\rho_I c_I)}(1 - \Re) = \frac{1}{(\rho_{II} c_{II})}\mathbf{T} \quad . \qquad \text{(A2)}$$

Solving for $\Re$ and **T**, we have

$$\mathbf{T} = \frac{2Z_{II}}{Z_I + Z_{II}} \quad \& \quad \Re = \frac{Z_{II} - Z_I}{Z_I + Z_{II}} \quad . \qquad \text{(A3)}$$

Various combinations of relative values of Z_I and Z_{II} help define different kinds of boundaries with specific characteristics.

1. When $Z_I = Z_{II}$, $\mathbf{T} = 1$ & $\Re = 0$: This means that the entire incident wave is transmitted to the other medium and there is no reflection. This situation is called *impedance matching* between the two media.
2. For $Z_{II} \gg Z_I$, $\Re \approx 1$: This kind of boundary is called a *rigid boundary*. In this case, the entire wave is reflected back into the first medium and practically no transmission occurs.
3. In case $Z_I \gg Z_{II}$, $\Re \approx -1$: This kind of boundary is called a *pressure release boundary*. In this case as well, there is practically no transmission, and the entire wave is reflected back into the first medium. However, an interesting feature of this kind of boundary is that the incident wave is inverted after reflection, *i.e.*, it is out of phase by 180°.

Literature Cited

1. Beranek, L. L., Acoustical Properties of Homogeneous, Isotropic Rigid Tiles and Flexible Blankets, *J. Acoust. Soc. Am.* **19**(4), 556–568 (1947).
2. Beranek, L. L., "Acoustical Measurements," Wiley, NY, 1949.
3. Bies, D. A., Acoustical Properties of Porous Materials, in "Noise and Vibrations Control," L. L. Beranek, Ed., McGraw Hill, NY, 1971, pp. 245–269.
4. Datar, G. V., Banks-Lee, P., and Grady, P. L., Acoustical Characteristics of Fabrics in High Intensity Ultrasound, *Appl. Acoust.* **48**(1), 33–45 (1996).
5. Datar, G. V., Banks-Lee, P., and Grady, P. L., Acoustical Characteristics of Fabrics in Low Intensity Ultrasound, *Appl. Acoust.* **47**(4), 345–350 (1996).
6. Ensminger, D., "Ultrasonics: Fundamentals, Technology, Applications," Marcel Dekker Inc., NY, 1988, pp. 139–175.
7. Fyrillas, M., and Szeri, A. J., Dissolution or Growth of Soluble Spherical Oscillating Gas Bubbles, *J. Fluid Mech.* **277**, 381–407 (1994).
8. Gooijer, H., Flow Resistance of Textile Materials, Doctoral thesis, University of Twente, 1998.
9. McCall, R. E., Lee, E. R., Mock, G. N., and Grady, P. L., Improving Dye Yields of Vats on Cotton Fabric Using Ultrasound, in AATCC International Conference & Exhibition 1998—Book of Papers, pp. 188–194.
10. Moholkar, V. S., "Intensification of Textile Treatments: Sonoprocess Engineering," Twente University Press, Enschede, 2002.
11. Moholkar, V. S., and Warmoeskerken, M. M. C. G., Mechanistic Aspects and Optimization of Ultrasonic Washing, *AATCC Rev.* **2**(2), 34–37 (2002).
12. Nichols, R. H. Jr., Flow Resistance Characteristics of Fibrous Acoustical Materials, *J. Acoust. Soc. Am.* **19**(5), 866–871 (1947).
13. Pierce, A. D., "Acoustics: An Introduction to Its Physical Principals and Applications," Acoustical Society of America, NY, 1989, pp. 140–148.
14. Prospreretti, A., and Commander, K. W., Linear Pressure Waves in Bubbly Liquids: Comparison Between Theory and Experiment, *J. Acoust. Soc. Am.* **85**(2), 732–746 (1989).
15. Rathi, N. H., Mock, G. N., McCall, R. E., and Grady, P. L., Ultrasound Aided Open Width Washing of Mercerized 100% Cotton Twill Fabric, in "AATCC International Conference & Exhibition 1997—Book of Papers," pp. 254–262.

16. Shah, Y. T., Pandit, A. B., and Moholkar, V. S., "Cavitation Reaction Engineering," Plenum Press, NY, 1999.
17. Suslick, K. S., "Ultrasound: Its Chemical, Physical and Biological Effects," VCH Publishers, NY, 1988.
18. van den Brekel, L. D. M., Hydrodynamics and Mass Transfer in Domestic Drum-type Fabric Washing Machines, Doctoral thesis, Technical University of Delft, 1988.
19. Vér, I. L., and Holmer, C. I., Interaction of Sound Waves with Solid Structures, in "Noise and Vibrations Control," L. L. Beranek, Ed., McGraw Hill, NY, 1971, pp. 270–361.
20. Yachmenev, V. G., Blanchard, E. J., and Lambert, A. H., Study of the Influence of Ultrasound on Enzymatic Treatment of Cotton Fabric, *Textile Chem. Color. Am. Dyest. Rep.* **1**(1), 47–51 (1999).
21. Yachmenev, V. G., Blanchard, E. J., and Lambert, A. H., Use of Ultrasound Energy in the Enzymatic Treatment of Cotton Fabric, *Ind. Eng. Chem. Res.* **37**(10), 3919–3923 (1998).
22. Zwikker, C., and Kosten, C. W., "Sound Absorbing Materials," Elsevier Science, London, 1949.

Manuscript received October 2, 2002; accepted December 5, 2002.

Variations in Sensibility to Fabric Frictional Sound by Fiber Type and Subject

YOUNGJOO NA

Department of Clothing & Textiles, Inha University, Inchon, South Korea

GILSOO CHO

Department of Clothing & Textiles, Yonsei University, Seoul, South Korea

ABSTRACT

We have investigated sensation responses to fabric frictional sounds according to fiber type, subject's nationality, age, gender, and acoustic sensitivity. Twenty-six American and thirty-two Korean adults participated in this study, and answered questions on seventeen adjectives describing sensations upon hearing the frictional sounds of eight fabrics, including "feeling good," "harsh to ear," "sharp," "deep," "loud," and "strong," etc. The structural concept of sound sensation has four dimensions: "height," "feeling good," "dimension," and "rustling." Americans identified the sound of wool fabric better than Koreans, while Koreans identified the sound of silk fabric better than Americans. The percent contributions of five variables of subject and fiber type to each sound sensation were calculated by ANOVA. Fiber type affected the four sound sensations most, followed by the subject's age and nationality. Other variables were hearing sensitivity and subject's gender.

Clothing comfort is related to the subjective perception of various sensations. The brain's psychological processes form subjective perceptions of sensory sensations from neurophysiological sensory signals, then formulate subjective overall perceptions and preferences by evaluating and weighting various sensory perceptions against past experiences and internal desires. By neurophysiological mechanisms of the sensory reception system in the skin, eyes, and other organs, the sensory signals are formulated from the interactions of the body with the clothing and the surrounding environment [7]. The brain does not perceive the comfort world as a series of independent sensory experiences, but instead, different sensory impressions mix to subtly alter and integrate sensory components [15].

Although many sensory studies [1, 10, 14] have dealt with tactile and visual comfort factors, studies of acoustic comfort are rare. Acoustic energy through a fabric is caused by the oscillation of air molecules, and how much this oscillation is impeded by barriers governs the acous-